

Article

Settling of Iron and Aluminum Particles in Acid Solutions for Acid Drainage Remediation

Paula Guerra ^{1,*} , Julio Valenzuela ², Consuelo Rámila ³ and Giannina Cattaneo ¹

¹ Departamento de Ingeniería Química y Ambiental, Universidad Técnica Federico Santa María, Avenida Vicuña Mackenna 3939, San Joaquín, Santiago 7820436, Chile; cattaneo.giannina@gmail.com

² Departamento de Ingeniería Metalúrgica y Minas, Universidad Católica del Norte, Avenida Angamos 0610, Antofagasta 1240000, Chile; jvalenzuela01@ucn.cl

³ Independent Researcher, Santiago 7750000, Chile; consueloramila@gmail.com

* Correspondence: paula.guerra@usm.cl; Tel.: +56-2-2303-7302

Abstract: Mineral processing is intensive in water usage. Unfortunately, a large portion of this valuable asset is contaminated by toxic species that leach from tailings or mineral ore, leading to the formation of acid drainage. Water from acid drainages can still be recovered by passive environmentally friendly treatments. An underestimated passive treatment is the settling of harmful metals, such as iron and aluminum. In this sense, floc settling from acid drainage has not been well studied. The objective of this work is to research the phenomena governing iron and aluminum floc settling in acid drainage, particularly, the chemical conditions that promote settling. The settling velocity of iron and aluminum flocs was studied in a column at different pH and iron/aluminum concentrations. Stability was studied through zeta potential. According to the results, iron flocs settle faster than aluminum and aluminum+iron (mixed) flocs, and a lower pH promotes a higher settling velocity and greater floc stability, which a lower zeta potential (which favors aggregation) allows for. The results improve the understanding of the interactions between the chemical and physical processes involved in floc settling, which, in turn, can improve the optimization of water treatment design. Future experiments must include particle size distribution, floc porosity, and effective particle density of iron and/or aluminum particles in acid waters.

Keywords: acid mine drainage; passive treatment; aluminum; iron; flocs; settling velocity; pH effect; zeta potential



Citation: Guerra, P.; Valenzuela, J.; Rámila, C.; Cattaneo, G. Settling of Iron and Aluminum Particles in Acid Solutions for Acid Drainage Remediation. *Water* **2022**, *14*, 2231. <https://doi.org/10.3390/w14142231>

Academic Editor: Qicheng Feng

Received: 31 May 2022

Accepted: 7 July 2022

Published: 15 July 2022

Publisher's Note: MDPI stays neutral with regard to jurisdictional claims in published maps and institutional affiliations.



Copyright: © 2022 by the authors. Licensee MDPI, Basel, Switzerland. This article is an open access article distributed under the terms and conditions of the Creative Commons Attribution (CC BY) license (<https://creativecommons.org/licenses/by/4.0/>).

1. Introduction

Acid mine drainage or acid rock drainage constitute water sources of depleted quality. Acid drainage is formed by the release of sulfate, acidity, and toxic elements into the environment by environmentally exposed sulfide-bearing minerals (mineral ore and tailings) [1]. Despite its poor quality, it is still considered a valuable water resource, especially in water-scarce industrialized areas [1].

Acid drainage can be treated using active and passive systems. Active treatments include chemical precipitation, reverse osmosis, solvent extraction, adsorption, and ion exchange [1]. Although effective, these technologies are intensive in energy, maintenance, and reagent consumption [1,2]. Passive treatments, which rely on natural processes, present much lower operating costs and environmental impacts due to their lower energy and reagent requirements. Therefore, passive treatment are valuable options for treating or pre-treating acid drainage [3,4].

One alternative passive treatment to remove metals and toxic trace elements from the aqueous phase in systems affected by acid drainage is the settling of iron and aluminum precipitates [3,5]. Iron secondary mineral phases, such as jarosite, schwertmannite, and ferrihydrite, precipitate from pH values as low as 2.0 [6]. At pH values of 4.5, aluminum phases such as gibbsite, hydrobasaluminite, and basaluminite precipitate [7–9]. These iron

and aluminum phases provide reactive surfaces for the adsorption or co-precipitation of toxic trace elements such as arsenic, zinc, lead, cadmium, and copper, among others [10–14]. Iron and aluminum precipitates can aggregate into flocs, which can subsequently settle removing the adsorbed/co-precipitated contaminants.

Iron and aluminum precipitates are naturally present in high quantities in the sediments of riverine systems affected by acid drainage [15,16]. Ochre-colored sediments, characteristic of iron oxyhydroxides, and white precipitates, characteristic of aluminum oxyhydroxides, enriched in trace elements, form part of the fine sediment on stream beds of various sites affected by acid drainage [17–23]. The settling of these phases significantly reduces the pollutant flux in these water bodies [19,24], constituting a key process in these systems.

Despite its importance, aluminum and iron flocs' settling behavior in systems affected by acid drainage (or in acid sulfate waters) is poorly understood. Particle size distribution (PSD) in sites affected by acid drainage has only recently been studied [14,19,25,26]. The first study model was the Caracarani River (pH 8.6)—Azufre River (pH 1.9) confluence [19,25,26]. This is a system affected by acid mine drainage, located in the Lluta River basin, Chile. In these studies, the authors analyzed PSD in situ, at several locations downstream of the confluence. They also analyzed PSD at the laboratory where different ratios of the rivers were mixed. Studies showed that PSD was affected by organic matter [26] and pH [25,26]. Therefore, it was hypothesized that these parameters would affect the settling velocity of flocs [26]. However, no settling experiments or in situ settling velocity measurements were performed. In another study, Montecinos et al. [14] studied PSD downstream the San Francisco River and Yerba Loca River, both strongly affected by copper mining sites located upstream. They applied the adapted Stokes' law (as done by other authors [27]) to estimate floc settling velocities from empirical data, i.e., floc size distribution, volumetric concentration, and total suspended solids concentration [14]. Although floc size is of great importance, these are not the only characteristics that determine their settling behavior, which are not considered in settling models such as the Stokes' law [28,29]. Therefore, the effect of water quality and pH on the actual settling behaviour of aluminum and iron flocs in acid waters is still uncertain.

Iron and aluminum particles formed in acid sulfate waters depend on the redox potential, pH, and composition of the solution (e.g., the concentration of iron, aluminum, sulfate, chloride, and carbonate) [30]. Depending on these factors, iron and aluminum will form oxides, oxyhydroxides, and/or hydroxysulfate minerals [31]. Solutions composition (e.g., ionic strength, cations and anions type, and concentration) and pH also affect flocculation. The first step in this process is the destabilization of particles. In this step, electrostatic repulsive forces between particles must be reduced to allow their aggregation by van der Waals attractive forces. Minimum repulsive forces occur at the particles' pH of zero charge (pH_{zc}), where the net charge of their surface (zeta potential) is 0 mV [32]. Repulsive forces decrease at high ionic concentrations due to the compression of the electrical double layer that surrounds the particles. Once destabilization is achieved, particles can adhere to each other, leading to the formation of flocs and their subsequent settling. If destabilization is inadequate, the settling process can be drastically affected [32]. Consequently, pH determines the type of primary particles that will form the flocs and also affects the flocculation process. Therefore, it could significantly impact flocs' settling dynamics in acid waters.

Acid mine drainage impacted systems generally present high concentrations of both aluminum and iron. When present together, these two metals interact. For example, aluminum (III) can coprecipitate with iron oxyhydroxides, such as ferrihydrite, when acid mine drainage is neutralized [33,34]. Aluminum can incorporate into ferrihydrite structure by substituting iron(III) [33]. This can modify the surface properties of ferrihydrite, for example, via increasing its pH_{zc} [35]. Additionally, if aluminum coprecipitates with ferrihydrite, a smaller amount of aluminum minerals will be formed, which could lead to the formation of smaller flocs. Hence, iron flocs could change their settling behavior due to the presence of aluminum and vice versa. The pH range where iron and aluminum

precipitate simultaneously is 4.5 and above (at pH below 4.5, there is no precipitation of aluminum phases) [6], therefore it is important to study this pH range to analyze possible interactions.

Settling of iron and aluminum particles in acid waters is relevant for a better understanding of the fate of contaminants and to improve the design of settling infrastructure, considering not only the physical but also the chemical composition of acid waters. Iron and aluminum particles frequently co-exist in acid waters, and their physical interactions have been addressed only recently [14,19,25,26]. Do iron and aluminum mixtures enhance or hinder settling in acid waters? What is the effect of iron and/or aluminum concentrations in floc settling? Does pH play a role in settling behavior?

The hypothesis of this work is that the settling behavior of acid mine drainage flocs is dependent on pH and on iron and aluminum presence. To assess this hypothesis, the objective of this study was to evaluate how bulk settling velocity in synthetic acid drainage solutions is modified, depending on the pH and the iron and aluminum presence. Some possible explanations for the observed effects were explored, investigating changes in: (i) the potential mineral phases formed (through geochemical modeling) and (ii) the colloid stability (through zeta potential measurements). This work is a first approximation to how bulk settling of acid drainage flocs can be improved by modifying chemical conditions, with the goal of improving remediation processes.

2. Materials and Methods

2.1. Preparation of Synthetic Acid Drainage

Six synthetic acid drainage solutions with different aluminum and iron concentrations were prepared. To do this, the following reagents were added to deionized water: $\text{Al}_3(\text{SO}_4)_2 \cdot 18 \text{H}_2\text{O}$, $\text{FeCl}_3 \cdot 6\text{H}_2\text{O}$, H_2SO_4 98% *w/w* to adjust SO_4^{2-} final concentration, and NaCl to adjust Na^+ and Cl^- final concentrations. Then, aliquots of NaOH 2 M were added to adjust pH to a final value of 2.

Two sets of solutions were prepared: (i) 50 mg/L metal concentrations, with an estimated ionic strength of 0.11 M; and (ii) 100 mg/L metal concentrations, with an estimated ionic strength of 0.13 M. These concentrations were selected based on the observations of the Azufre River–Caracarani River confluence, Northern Chile [19]. An additional reason to select concentrations based on this specific site is because of the formation of ochre and opalescent particles, attributable to iron and aluminum flocs, both suspended and as part of the stream bed [19], which are also frequently observed at other sites affected by acid drainage [6–8,10]. Iron and aluminum concentrations can vary from site to site; the concentrations (in Table 1) were selected as a first approach towards understanding iron and aluminum particle settling in acid waters. Their detailed composition is presented in Section S1 of the Supplementary Material.

Table 1. Synthetic acid drainage solutions composition.

Solution	Fe ³⁺ (mg/L)	Al ³⁺ (mg/L)	SO ₄ ²⁻ (g/L)	Ionic Strength (M)
100 mg Fe/L	100	0	2.4	0.13
100 mg Al/L	0	100	2.4	0.13
100 mg Fe/L + 100 mg Al/L	100	100	2.4	0.26
50 mg Fe/L	50	0	2.4	0.11
50 mg Al/L	0	50	2.4	0.11
50 mg Fe/L + 50 mg Al/L	50	50	2.4	0.22

Solid reagents were weighed in using a precision scale (± 0.0001 g; RadWag, model PS 510/C/1, Miami, FL, USA). The pH of the solutions was measured with the pH-meters: HANNA HI2020, Woonsocket, RI, USA or JENCO, 6010 M, San Diego, CA, USA (according to equipment availability at the time of the experiment). The HANNA pH-meter was calibrated by using buffers of pH 4, 7 and 10. The JENCO pH-meter was calibrated by using buffers of pH 4 and 7. All reagents used were analytical grade.

2.2. Mixing, Coagulation, and Flocculation for the Formation of Iron and Aluminum Floccs

Iron and aluminum phases were precipitated by adjusting the pH of the synthetic acid drainage solutions (Table 1) to 4.5, 5.5, and 6.5 with NaOH 2 M. Immediately after this, each suspension was stirred in 2 L beakers of a Jar Test apparatus (JL6, VELP SCIENTIFICA, Usmate, Italy) following a coagulation–flocculation sequence. The coagulation stage consisted of stirring the mixture at 300 rpm during 30 s, and the following flocculation stage consisted of stirring at 50 rpm during 30 min (procedure adapted from [36]).

2.3. Settling Column Tests

2.3.1. Settling of Freshly Formed Floccs

Immediately after the coagulation–flocculation process finished, the suspensions were carefully poured into acrylic columns for settling. Each floc suspension was left to settle for 120 min. The length of the column (L) was 350 mm or 400 mm (see Section S2 of the Supplementary Material) with a square cross-section of $65 \times 65 \text{ mm}^2$. The six solutions presented in Table 1 were tested at three pH levels (4.5, 5.5, and 6.5), and each settling experiment was made in duplicate (total $n = 36$). All experiments were performed at room temperature ($\sim 20^\circ\text{C}$).

The interface height between the floc phase and the clarified phase (H) was measured from bottom to top, by placing a graduated tape measure on the side of the settling column. Measurements were performed at 14 time intervals (t): 0, 2.5, 5, 10, 15, 20, 30, 40, 50, 60, 70, 80, 90, and 120 min. We assumed dispersed settling occurred throughout the whole settling process according to Kynch's theory [37]. However, we observed that it was difficult to clearly identify the floc phase–clarified phase interface, especially during the first few minutes (see Section S2 of the Supplementary Material), so hindered settling may have occurred in some areas of the column [38–40]. Bhargava [41] found that the upper limit value for hindered settling is 0.5 g/L for aluminum, while the limit value is 1 g/L for iron. This means that van der Waals forces may have affected the settling process due to additional particle interaction or particle interference at some point. Regardless, this simple procedure allowed us to perform a semi-quantitative exploration which allowed to compare the settling behavior of iron and aluminum suspensions in acid solutions.

2.3.2. Settling Velocity Determination

The settling velocity of the interface (V_s) was calculated as the maximum dH/dt value [42]. To do this, we fitted a fine time-grid with $\Delta t = 7.2 \text{ s}$ was fitted to the measured interface height using a shape-preserving piecewise cubic interpolation [43]. Time derivative was computed over this higher resolution grid, where V_s occurred when the derivative reached its maximum value. Significant differences between experimental results were measured through analysis of confidence intervals with an $\alpha = 0.05$.

2.4. Geochemical Modeling

To identify the possible mineral phases that could precipitate in each solution, and to estimate their ionic strength (IS, presented in Table 1), geochemical modeling was performed using the USGS PHREEQC code, version 3.6.2, Reston, VA, USA. We used the wateq4f.dat database, as it is the most appropriate for systems associated with acid drainage [44]. Additional reactions for schwertmannite [45] and hydrobasaluminite [7] were added to the code, as they do not form part of the wateq4f.dat database.

Schwertmannite, $\text{Fe}(\text{OH})_3(\text{a})$, hydrobasaluminite, and $\text{Al}(\text{OH})_3$ were the iron and aluminum phases chosen to precipitate in the simulations. These meta-stable phases were selected, as they are the most probable minerals to rapidly form in systems affected by acid mine drainage, at the pH range studied (pH 4.5–6.5) [7,34,45,46]. Hydrobasaluminite was preferred to basaluminite because the latter is formed by the dehydration of hydrobasaluminite [34], a process that is not expected in our suspensions.

The conceptual model consisted of mixing each solution described in Table 1 (Solution 1) with a fraction of NaOH 2 M solution (Solution 2) until pHs of 4.5, 5.5, and 6.5 were

reached. Solutions were mixed in the following ratios: Solution 1 = 0.999 + Solution 2 = 0.001, (. . .) to Solution 1 = 0.960 + Solution 2 = 0.040. At first, the solution fraction discretization was 0.001. Several iterations were then performed with smaller discretization (0.00001, 0.000001) until reaching the desired pH value. Simulations were performed assuming $T = 20\text{ }^{\circ}\text{C}$ and equilibrium with respect to atmospheric O_2 and CO_2 . An example of the code used is presented in Section S3 of the Supplementary Material.

2.5. Zeta Potential Measurements

Electrokinetic characterizations were performed on the two 50 mg/L suspensions (50 mg Al/L, 50 mg Fe/L) and one 50 mg Al/L + 50 mg Fe/L, within a pH range of 4.5 to 8.5. Two replicas of each measurement were performed. The solutions were prepared as described in Section 2.1. Then, aliquots of NaOH or HCl 0.01 M were added to 100 mL of the solutions to adjust pH (measured with a pH-meter HANNA HI5521, Woonsocket, RI, USA) and were stirred using a magnetic agitator (100 rpm; BOECO MSH-420, Hamburg Germany). Zeta potential experiments were not performed on 100 mg/L as iron and/or aluminum concentrations formed much thicker flocs.

The electrokinetic characterization was carried out using the direct current (DC) electrophoretic mobility method with the Malvern Zetasizer NanoZS90 (Malvern Instruments, Malvern, UK). The instrument was calibrated at $25\text{ }^{\circ}\text{C}$, and its accuracy was $\pm 10\%$. There were two replicas per measurement.

3. Results

3.1. Settling Tests

The evolution of the clarified-interphase heights (H) in the settling column tests, normalized by the corresponding column height (L), are presented in Figure 1. Floc settling occurred faster in iron suspensions and the pH affected the shape of settling curves. The effect of pH on settling curves is especially evident for 100 mg/L suspensions when aluminum is present. A significant shift can be observed in 100 mg/L aluminum and mixed suspensions between pH 4.5 and pH 6.5 (Figure 1c,e, respectively). Although less pronounced, this phenomenon can also be noticed for the 50 mg/L aluminum and mixed suspensions (Figure 1d,f, respectively).

Settling Velocity

Iron and aluminum suspensions V_s are presented in Figure 2 (see Section S4 of Supplementary Material for detailed data). V_s was within the range of 0.61–1.61 mm/s and 0.29–1.89 mm/s for the 50 mg/L (Figure 2a) and 100 mg/L (Figure 2b) suspensions, respectively (Figure 2). The mean V_s for 50 mg/L suspensions was 1.19 ± 0.28 mm/s ($n = 18$), while the mean V_s for 100 mg/L suspensions was 0.96 ± 0.61 mm/s ($n = 18$). These V_s values are similar to those previously reported for iron and aluminum hydroxide flocs (e.g., 0.52 mm/s and 0.33 mm/s, respectively [41]); although strict comparisons cannot be made because flocs settling in acid sulfated water has not been evaluated before.

Iron suspensions tended to present the highest V_s in all experiments (0.90–1.89 mm/s), or a mean $V_s = 1.42 \pm 0.30$ mm/s ($n = 12$). Confidence interval analysis shows that V_s of iron suspensions was significantly higher than Al + Fe mixed suspensions (0.83 ± 0.35 mm/s, $n = 12$) and Al = 100 mg/L suspension of pH 5.5 and 6.5 (0.32 ± 0.02 mm/s, $n = 4$) (Figure 2). The density of iron phases is higher than aluminum phases, which explains the higher settling velocity. The mixed phases present lower velocities due to the presence of less dense aluminum phases.

The settling velocity was only higher at pH 4.5 for Al = 100 mg/L suspension and for the mixed iron and aluminum suspension (100 mg/L Al + 100 mg/L Fe); the rest of the suspensions did not present any significant differences. This is a strong indication that iron and aluminum concentration is a more controlling factor than pH in settling velocity.

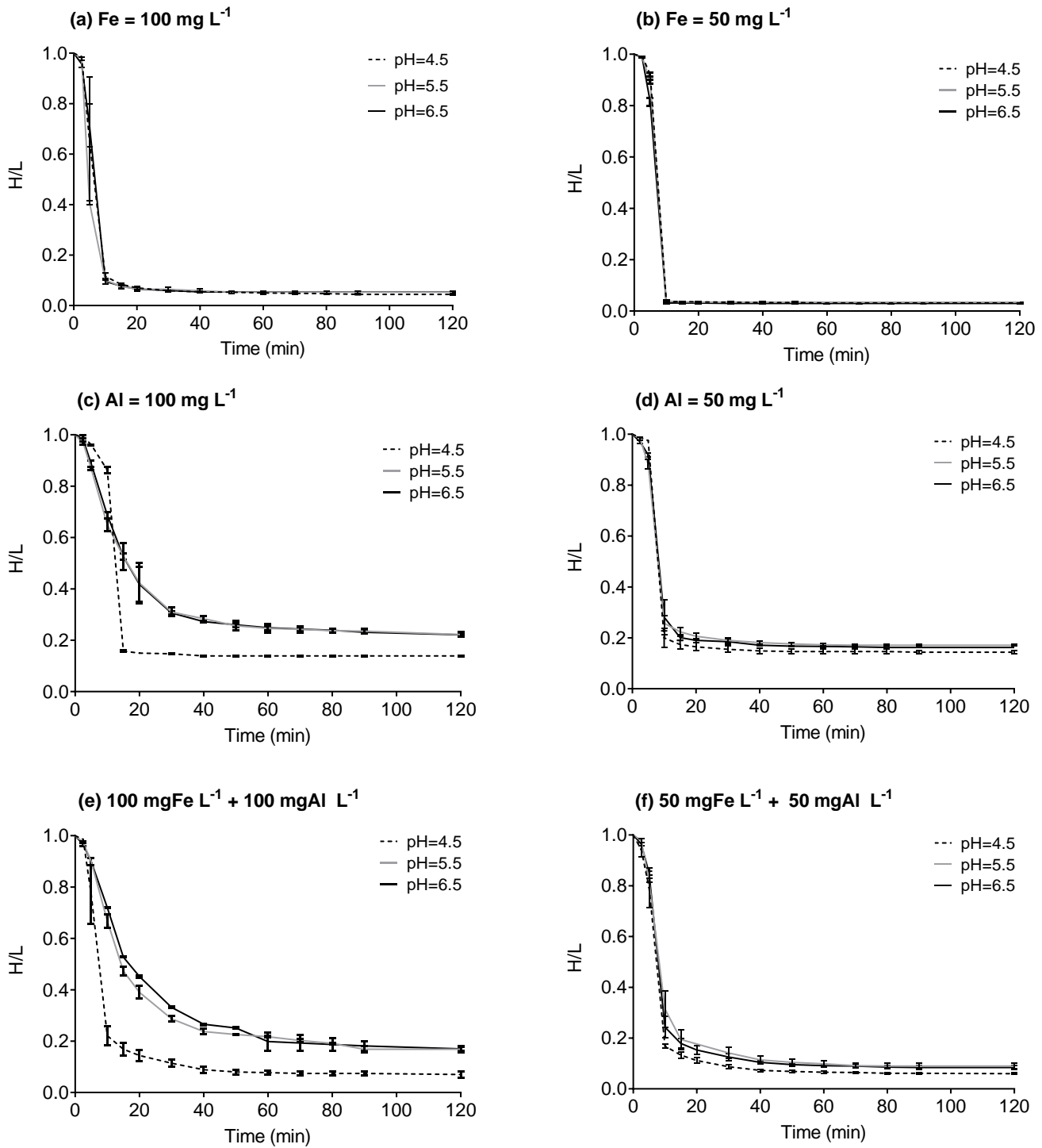


Figure 1. Floc phase-clarified phase settling height (H) of iron, aluminum, and iron+aluminum suspensions standardized by column height (L) (mean and range).

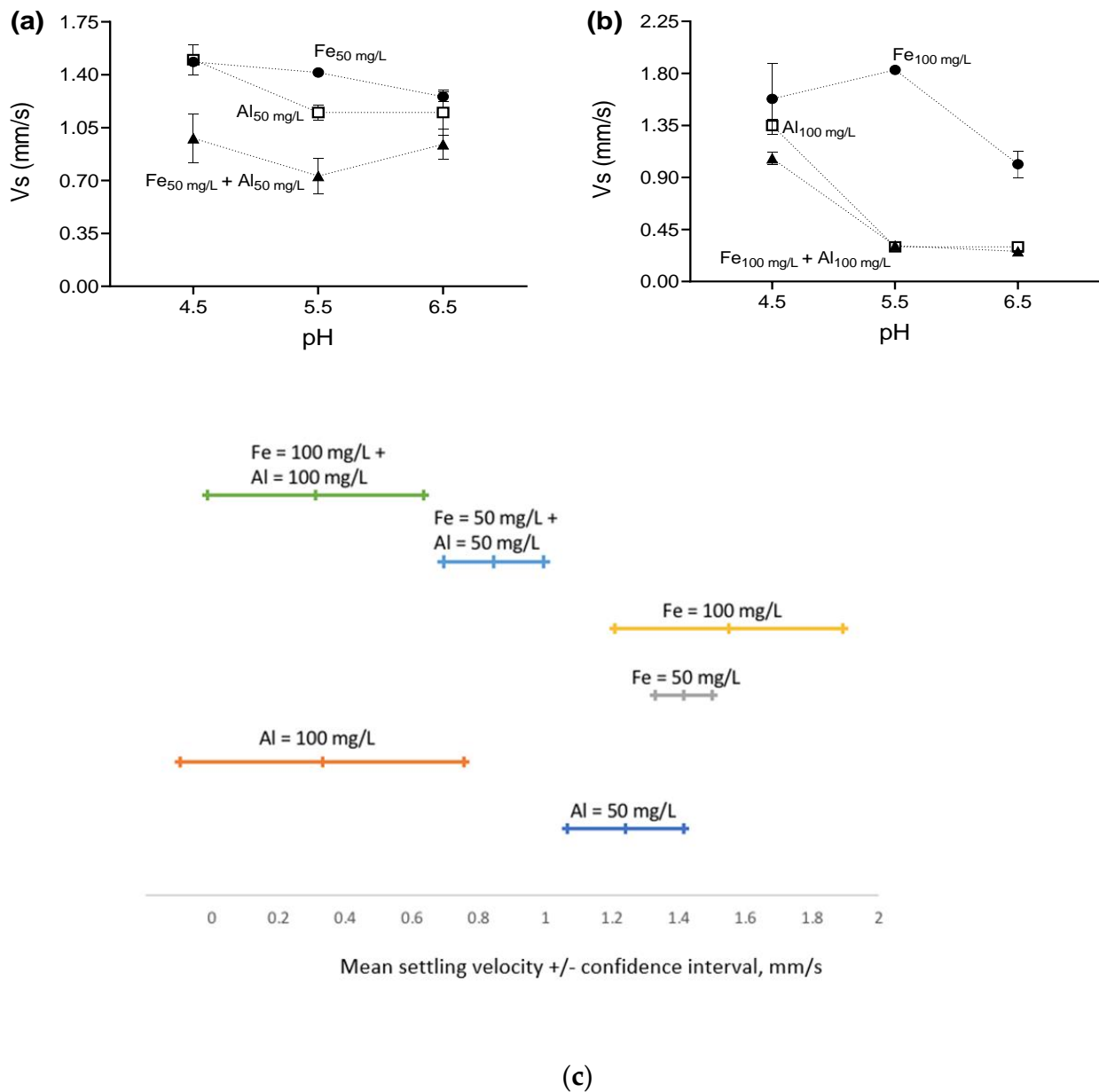


Figure 2. Settling velocity of the interface (V_s : mean and range) at the three pH levels evaluated. (a) Suspensions with metal concentrations of 50 mg/L. (b) Suspensions with metal concentrations of 100 mg/L. (c) Confidence intervals with $\alpha = 0.05$.

As for the effect of aluminum concentration on settling velocity, lower aluminum concentration presented a higher settling velocity than higher aluminum concentration (1.24 ± 0.22 mm/s and 0.33 ± 0.53 mm/s, respectively). In compression settling, the higher the concentration, the higher the settling velocity. In this case, settling does not respond to compression settling; there are certain interactions (floc formation, water absorption) that hinder the settling process. This indicates that there is an important difference between iron and aluminum floc structure in acid waters. No significant difference between lower concentration and higher concentration solutions was observed for iron suspensions.

A significant difference between the settling velocities of individual iron and aluminum solutions was observed for 100 mg/L solutions. The V_s of 100 mg/L iron solutions was 1.55 ± 0.42 (n = 6) and the V_s of 100 mg/L aluminum solution was 0.33 ± 0.54 mm/s (n = 6). This is attributable to the higher density of iron phases compared to the lower

density of aluminum phases. However, no significant difference was observed between individual lower concentration iron and aluminum solutions.

3.2. Geochemical Modeling

Simulations showed that the mineral phases that could precipitate in the synthetic acid drainage solutions were amorphous $\text{Fe}(\text{OH})_3$ and hydrobasaluminite, while schwertmannite and $\text{Al}(\text{OH})_3$ would not reach their saturation point in any solution (Figure 3). Minerals would precipitate at higher amounts in solutions with higher metal concentrations: 0.175 vs. 0.088 mmol/L for amorphous $\text{Fe}(\text{OH})_3$ (Figure 3a,b, respectively) and 0.91 vs. 0.45 mmol/L for hydrobasaluminite (Figure 3c,d, respectively), as expected. The pH did not vary significantly between the preparation of solutions (right before coagulation–flocculation), after coagulation–flocculation, and finally after 20 min of settling. This means variation in precipitates is not expected.

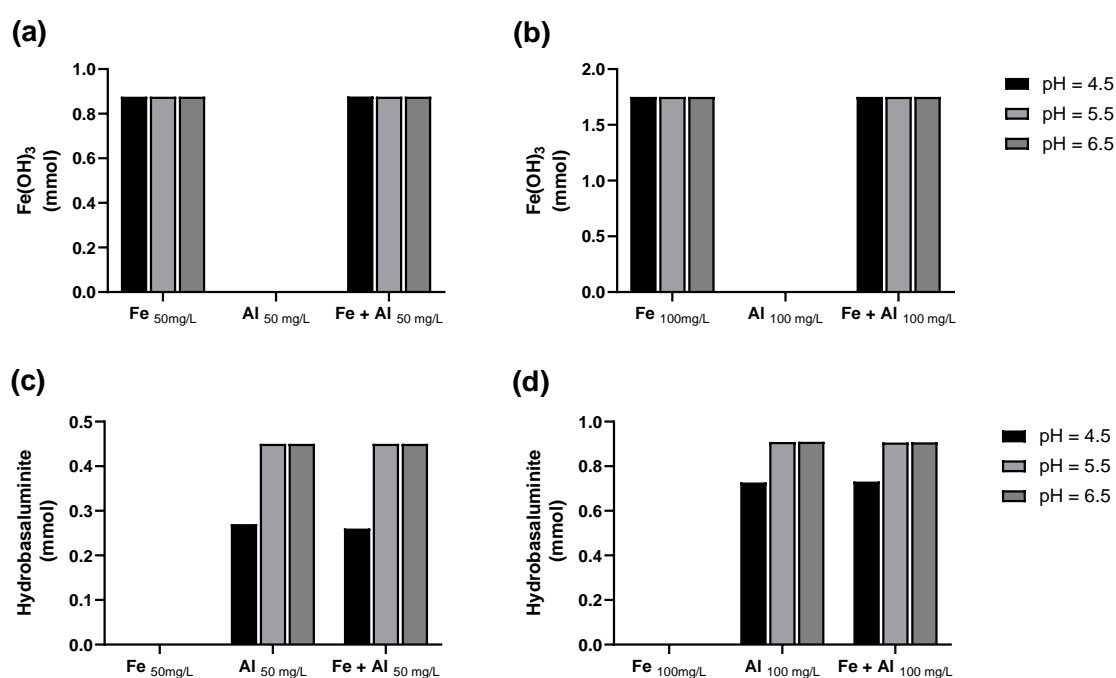


Figure 3. Iron and aluminum mineral phases precipitated according to geochemical simulations. (a,b) Amorphous $\text{Fe}(\text{OH})_3$ precipitated equally at the three pH levels studied in iron and mixed solutions; (c,d) Hydrobasaluminite precipitation was lower at pH = 4.5, precipitating at the same levels in aluminum and mixed solutions.

The pH would not affect iron precipitation, as the same amount of amorphous $\text{Fe}(\text{OH})_3$ precipitated at the three pH levels (Figure 3a,b). Hydrobasaluminite formation, on the other hand, was affected by the pH, precipitating at lower amounts at pH 4.5 (Figure 3c,d). The fraction of aluminum that did not precipitate at pH 4.5 would be mostly present as AlSO_4^+ complex (see Section S5 of Supplementary Material). Simulated mixed acid drainage solutions showed the same amount of precipitation as iron and aluminum solutions for both, hydrobasaluminite and amorphous $\text{Fe}(\text{OH})_3$. Therefore, aluminum did not interfere with iron precipitation or vice versa.

These simulations must be considered as a first approximation. These do not consider, for example, reactions of coprecipitation or adsorption. Therefore, potential interactions between iron and aluminum cannot be completely observed. On the other hand, simulations are performed at complete thermodynamic equilibrium, and therefore do not consider the kinetics of the reactions. However, this should not be a major restriction, as $\text{Fe}(\text{OH})_3$ and hydrobasaluminite are known to form rapidly [7,47].

3.3. Zeta Potential Measurements

The particles presented a net negative surface charge across the entire pH range studied, going from -2.64 mV to -21.88 mV (see Section S6 of the Supplementary Material for detailed data). Surface charge decreased with increasing pH in all cases (Figure 4). However, the pHzc of the individual particles in the three suspensions was not attained, only for the whole suspension.

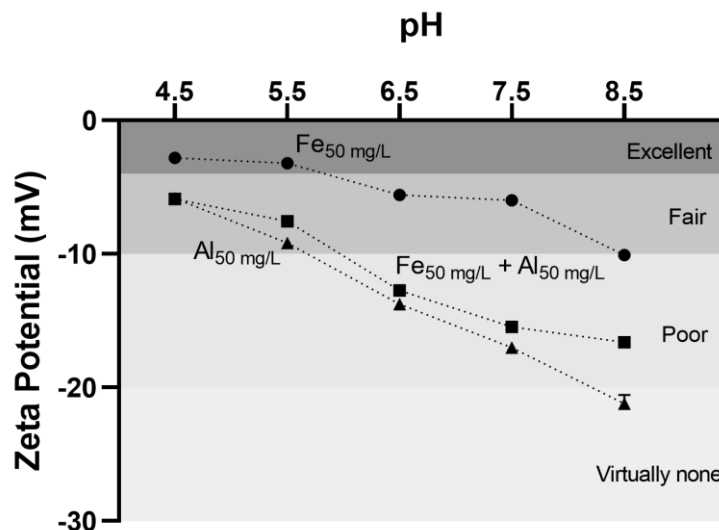


Figure 4. pH effect on zeta potential for iron, aluminum, and mixed suspensions (mean and range). Zones are colored according to the expected degree of coagulation of particles: excellent, fair, poor, and virtually none (categories proposed by [48]). Suspensions at lower pH are closer to the isoelectric point, within the zone of particle instability (excellent and fair areas).

Iron suspension presented the zeta potential values closest to 0 mV (Figure 4). The surface charge of particles in the iron solution was in the zone of “fair” (-10 to -3 mV) and “excellent” (-3 to 0 mV) degree of coagulation, throughout the entire pH range studied (according to the categories proposed by [48]).

Zeta potential in aluminum and mixed suspensions behaved similarly (Figure 4). At lower pH (4.5 and 5.5), their zeta potential reached the zone of “fair” degree of coagulation. At $\text{pH} \geq 6.5$ particles surface charge in both suspensions were within the zones of “poor” (-20 to -10 mV) and “virtually none” (-30 to -20 mV) degree of coagulation (Figure 4).

4. Discussion

In the following sections, the effect of pH and of iron/aluminum interference in the bulk settling behavior of synthetic acid drainage suspensions is discussed. Geochemical simulations results are used to explore if settling behavior could be explained, in part, by differences in the type and amount of primary particles formed under each condition. Zeta potential results are used to investigate if differences in the coagulation potential could explain the pH and iron/aluminum interference effects observed.

4.1. Iron Flocs Tend to Settle Faster Than Aluminum Flocs

Iron suspensions tended towards higher Vs (0.9 – 1.89 mm/s) than aluminum suspensions (0.29 – 1.61 mm/s) (Figure 2), although there was a degree of overlapping results. Differences between both are expected, as the types of flocs formed are different. Higher Vs in iron flocs can be attributed, in part, to the higher density of the mineral phases that form flocs: the density of iron (III) oxy/hydroxides range from 3.0 to 3.5 g/cm³ [49,50] while hydrobasaluminite has a density of 2.27 g/cm³ [51]. Settling velocity differences can also be explained by differences in the coagulation degree. Zeta potential is closer to 0 mV over the entire pH range for iron suspensions when compared with aluminum ones (Figure 4).

Therefore, iron particles were more destabilized than aluminum particles, which leads to better coagulation and flocculation.

Higher settling velocities observed in iron suspensions emphasize the importance of iron flocs in the removal of contaminants in acid waters. This goes in addition to their previously reported importance from the chemical perspective [19,52–56].

4.2. Mixed Suspensions Tended towards the Lowest Settling Velocities

Mixed suspensions presented the lowest V_s over the entire pH range (0.25–1.14 mm/s) (Figure 2). Within the experimental conditions of this study, the addition of aluminum resulted in lower settling velocities. In the case of the 100 mg/L suspensions, the interaction showed two behaviors. At pH 4.5, the V_s of mixed suspensions was lower than that of both iron and aluminum suspensions. However, at pH 5.5 and 6.5, the 100 mg Al/L and mixed suspensions presented the same behavior (Figure 1c,e) and V_s (Figure 2b). This suggests that aluminum flocs would be driving the settling of the mixed suspension at higher pHs, which can be explained by the presence of high amounts of hydrobasaluminite in both cases (Figure 3).

The differences observed between suspensions would not be explained by the formation or dissolution of the mineral phases simulated. According to geochemical simulations, the mineral phases formed were the same in type and quantity in mixed and in iron or aluminum solutions (Figure 3). Nevertheless, geochemical simulations do not consider other processes such as coprecipitation, which may have occurred [33,34]. This process could have modified the type of primary particles and therefore their characteristics. The higher concentrations of particles in mixed suspensions could be another possible explanation (Figure 3). As solid concentration increases, interactions between flocs also increase, which decreases V_s [41].

Zeta potential differences cannot explain the lower V_s observed in mixed suspensions compared to aluminum concentrations, but can explain the differences between mixed suspensions and individual iron suspensions. Highly charged flocs would cause repelling or lower particle aggregation, which would lead to less dense (less aggregated) flocs (Figure 4) in the case of mixed suspensions.

4.3. pH Influences Iron, Aluminum, and Mixed Suspensions Settling

Settling was affected by pH, especially in high-concentration aluminum suspensions and mixed higher concentration suspensions, being the highest at pH 4.5 (Figures 2 and 3). In the rest of the solutions, pH tended to present the highest values at pH 4.5.

Iron suspensions' settling dependence on pH could be explained, in part, by changes in the zeta potential of particles. Surface negative charge increased with pH, being in the category "excellent" at pH 4.5 and 5.5, and "fair" at pH 6.5 (Figure 4). This behavior is similar to that observed in V_s . V_s decreased with pH, presenting a more evident decrease between pH 5.5 and pH 6.5 (Figure 2). Changes in the type and quantity of the mineral phases precipitated would not explain V_s dependence on pH. According to geochemical simulations, amorphous $\text{Fe}(\text{OH})_3$ would be the only mineral phase precipitating across the entire pH range evaluated; and the same quantity would precipitate in every case (Figure 3a,b).

Aluminum solutions' settling dependence on pH would be explained mainly by changes in the amount of mineral phases precipitated. At pH 4.5 part of the aluminum remained in solution (mainly as AlSO_4^+ complex), while at pH 5.5 and 6.5 aluminum completely precipitated (Figure 3c,d). Therefore, at pH 5.5 and 6.5 more aluminum particles are available, which can aggregate forming larger flocs. The increase in the number of linkages produces flocs with higher porosities, which entrap water, decreasing their density [28]. The decrease in floc density could be, in part, explaining the effect of pH on settling behavior [28]. It is interesting to note that V_s was almost the same for pH 5.5 and 6.5 (Figure 2). This matches what was observed in geochemical simulations, where the same amount of hydrobasaluminite precipitated at these two pH levels (Figure 3c,e). A

much greater effect of pH on V_s was observed in the 100 mg Al/L suspension. This could be attributed to the presence of less dense flocs and also to an increase in the interaction between flocs [41]. Finally, the zeta potential of aluminum decreases with pH (Figure 4), which could further explain the effect of pH on V_s . Nevertheless, particle (iron and/or aluminum) concentration would be more crucial on V_s .

Mixed solutions' settling dependence on pH could be attributed to both changes in the coagulation potential (Figure 4) and in the amount of hydrobasaluminite precipitation (Figure 3c,d). The reasons for this are as those explained above. In the case of 100 mg/L mixed suspensions, as in the 100 mg Al/L suspensions, the effect of pH could be explained mainly by differences in hydrobasaluminite precipitation. This is because pH 5.5 and 6.5 presented the same settling behavior. Higher amounts of hydrobasaluminite (at pH 5.5 and 6.5) could lead to the formation of flocs with lower density and to the increase in flocs interactions, which would decrease V_s .

4.4. Colloid Instability in Synthetic Mine Drainage Solutions Is Higher under Acidic Conditions

The three suspensions approached the pH_{zc} at the lowest pH evaluated (4.5) (Figure 4). However, typically, the pH_{zc} of aluminum hydroxides ranges between 7 and 9, while pH_{zc} for iron precipitates ranges between 6 and 8.5. Lower pH_{zc} of iron hydroxides have been observed in acid drainage due to the presence of sulfate [57]; the pH_{zc} for the acid drainage solution (in presence of sulfate) was 4, compared to the pH_{zc} of 8 and in absence of sulfate. As for aluminum suspensions, the presence of $AlSO_4^+$ complexes may contribute to further neutralize surface charges, thus promoting coagulation.

It is important to indicate that the particles were not sonicated prior to zeta potential measurements, so additional iron and/or aluminum floc interaction may have affected pH_{zc} . This must be verified with further experiments.

5. Conclusions

This work explored the settling process of iron and aluminum phases in acid drainage. Although this work was performed in controlled laboratory conditions, it contributes to a better understanding of the dynamics of iron and aluminum flocs that form part of the fine suspended sediments in systems affected by acid drainage.

The hypothesis of our work was that "the settling behavior of acid mine drainage flocs is dependent on pH and on iron and aluminum presence". We verified this hypothesis; however, through the analysis of our experiments we realized that the method we used to measure the aqueous phase-floc phase interface was not the best, as the interface was not easy to distinguish due to the low floc concentration. Additionally, we assumed dispersed flocculation to analyze settling behaviour, and given the nature of the flocs, another type of settling, such as hindered settling, may have occurred. Nevertheless, as a first exploration to show the effect of pH and iron/aluminum presence on settling velocity, we can draw the following conclusions: (i) Settling velocity is mainly affected by iron and/or aluminum concentration, and the presence of individual iron or aluminum phases, or mixtures; (ii) pH affects settling velocity in aluminum or mixed iron/aluminum suspensions, which can be explained by the values of zeta potential; at lower pH values, zeta potential was less negative, which favors the particle aggregation process through coagulation–flocculation; (iii) the zeta potential was less negative in lower pH solutions; this is a necessary condition for the aggregation process to occur, due to the lowering of the repulsive forces between particles, which would explain why lower pH solutions also tended towards higher settling velocities.

Future research on the effect of water quality of acid waters, i.e., iron and/or aluminum concentration and pH on particle size distribution, floc density, floc porosity, among others, are relevant factors to address to better understand iron and/or aluminum particle settling in acid waters.

Supplementary Materials: The following supporting information can be downloaded at: <https://www.mdpi.com/article/10.3390/w14142231/s1>, Section S1: Synthetic acid drainage solutions composition; Section S2: Photographs of settling experiments; Section S3: PHREEQC Code; Section S4: Settling tests—raw data; Section S5: Results of PHREEQC simulations; Section S6: Zeta Potential Data.

Author Contributions: Conceptualization: P.G. and J.V.; data curation: P.G., G.C. and J.V.; formal analysis: P.G.; funding acquisition: P.G.; investigation: P.G., G.C. and J.V.; methodology: P.G., G.C. and J.V.; project administration: P.G.; resources: P.G. and J.V.; supervision: P.G.; validation: G.C.; visualization: P.G.; writing—original draft: P.G. and C.R.; writing—review & editing: P.G., C.R. and J.V. All authors have read and agreed to the published version of the manuscript.

Funding: This research was funded by ANID (Agencia Nacional de Investigación y Desarrollo) through FONDECYT (Fondo Nacional de Desarrollo Científico y Tecnológico), Chile, Fondecyt Iniciación en Investigación grant number 11180314 (2018–2020).

Acknowledgments: We acknowledge Jeamilette Mendoza and Roberto Paredes from the Departamento de Ingeniería Química y Ambiental of Universidad Técnica Federico Santa María, Fernanda Carrasco from the Departamento de Ingeniería Hidráulica y Ambiental of Pontificia Universidad Católica for their kind contributions in the development of experiments. We also acknowledge Christian González from Arizona State University for his contribution in data analysis.

Conflicts of Interest: The authors declare no conflict of interest. The funders had no role in the design of the study; in the collection, analyses, or interpretation of data; in the writing of the manuscript, or in the decision to publish the results.

References

1. Oyewo, O.A.; Agboola, O.; Onyango, M.S.; Popoola, P.; Bobape, M.F. Current Methods for the Remediation of Acid Mine Drainage Including Continuous Removal of Metals From Wastewater and Mine Dump. In *Bio-Geotechnologies for Mine Site Rehabilitation*; Elsevier: Amsterdam, The Netherlands, 2018; pp. 103–114. ISBN 9780128129869.
2. Fernando, W.A.M.; Ilankoon, I.M.S.K.; Syed, T.H.; Yellishetty, M. Challenges and Opportunities in the Removal of Sulphate Ions in Contaminated Mine Water: A Review. *Miner. Eng.* **2018**, *117*, 74–90. [[CrossRef](#)]
3. Skousen, J.; Zipper, C.E.; Rose, A.; Ziemkiewicz, P.F.; Nairn, R.; McDonald, L.M.; Kleinmann, R.L. Review of Passive Systems for Acid Mine Drainage Treatment. *Mine Water Environ.* **2017**, *36*, 133–153. [[CrossRef](#)]
4. Schwarz, A.; Nancucheo, I.; Gaete, M.A.; Muñoz, D.; Sanhueza, P.; Torregrosa, M.; Rötting, T.; Southam, G.; Aybar, M. Evaluation of Dispersed Alkaline Substrate and Diffusive Exchange System Technologies for the Passive Treatment of Copper Mining Acid Drainage. *Water* **2020**, *12*, 854. [[CrossRef](#)]
5. Hu, Y.; Li, Q.; Lee, B.; Jun, Y.-S. Aluminum Affects Heterogeneous Fe(III) (Hydr)Oxide Nucleation, Growth, and Ostwald Ripening. *Environ. Sci. Technol.* **2014**, *48*, 299–306. [[CrossRef](#)]
6. España, J.S. The Behavior of Iron and Aluminum in Acid Mine Drainage: Speciation, Mineralogy, and Environmental Significance. In *Thermodynamics, Solubility and Environmental Issues*; Elsevier: Amsterdam, The Netherlands, 2007; pp. 137–150.
7. Sánchez-España, J.; Yusta, I.; Diez-Ercilla, M. Schwertmannite and Hydrobasaluminite: A Re-Evaluation of Their Solubility and Control on the Iron and Aluminium Concentration in Acidic Pit Lakes. *Appl. Geochem.* **2011**, *26*, 1752–1774. [[CrossRef](#)]
8. Nordstrom, D.K. Hydrogeochemical Processes Governing the Origin, Transport and Fate of Major and Trace Elements from Mine Wastes and Mineralized Rock to Surface Waters. *Appl. Geochem.* **2011**, *26*, 1777–1791. [[CrossRef](#)]
9. Cánovas, C.R.; Peiffer, S.; Macías, F.; Olías, M.; Nieto, J.M. Geochemical Processes in a Highly Acidic Pit Lake of the Iberian Pyrite Belt (SW Spain). *Chem. Geol.* **2015**, *395*, 144–153. [[CrossRef](#)]
10. Carrero, S.; Pérez-López, R.; Fernandez-Martinez, A.; Cruz-Hernández, P.; Ayora, C.; Poulain, A. The Potential Role of Aluminium Hydroxysulphates in the Removal of Contaminants in Acid Mine Drainage. *Chem. Geol.* **2015**, *417*, 414–423. [[CrossRef](#)]
11. Lecomte, K.L.; Maza, S.N.; Collo, G.; Sarmiento, A.M.; Depetris, P.J. Geochemical Behavior of an Acid Drainage System: The Case of the Amarillo River, Famatina (La Rioja, Argentina). *Environ. Sci. Pollut. Res.* **2017**, *24*, 1630–1647. [[CrossRef](#)]
12. Runkel, R.L.; Bencala, K.E.; Kimball, B.A.; Walton-Day, K.; Verplanck, P.L. A Comparison of Pre- and Post-Remediation Water Quality, Mineral Creek, Colorado. *Hydrol. Processes* **2009**, *23*, 3319–3333. [[CrossRef](#)]
13. Sánchez-España, J.; Yusta, I.; Burgos, W.D. Geochemistry of Dissolved Aluminum at Low PH: Hydrobasaluminite Formation and Interaction with Trace Metals, Silica and Microbial Cells under Anoxic Conditions. *Chem. Geol.* **2016**, *441*, 124–137. [[CrossRef](#)]
14. Montecinos, M.; Coquery, M.; Alsina, M.A.; Bretier, M.; Gaillard, J.-F.; Dabrin, A.; Pastén, P. Partitioning of Copper at the Confluences of Andean Rivers. *Chemosphere* **2020**, *259*, 127318. [[CrossRef](#)] [[PubMed](#)]
15. Contreras, M.T.; Müllendorff, D.; Pastén, P.; Pizarro, G.E.; Paola, C.; Escauriaza, C. Potential Accumulation of Contaminated Sediments in a Reservoir of a High-Andean Watershed: Morphodynamic Connections with Geochemical Processes. *Water Resour. Res.* **2015**, *51*, 3181–3192. [[CrossRef](#)]

16. Menshikova, E.; Osovetsky, B.; Blinov, S.; Belkin, P. Mineral Formation under the Influence of Mine Waters (The Kizel Coal Basin, Russia). *Minerals* **2020**, *10*, 364. [[CrossRef](#)]
17. Carroll, K.C.; López, D.L.; Stoertz, M.W. Solute Transport at Low Flow in an Acid Stream in Appalachian Ohio. *Water Air Soil Pollut.* **2003**, *144*, 195–222. [[CrossRef](#)]
18. Consani, S.; Carbone, C.; Dinelli, E.; Balić-Žunić, T.; Cutroneo, L.; Capello, M.; Salviulo, G.; Lucchetti, G. Metal Transport and Remobilisation in a Basin Affected by Acid Mine Drainage: The Role of Ochreous Amorphous Precipitates. *Environ. Sci. Pollut. Res.* **2017**, *24*, 15735–15747. [[CrossRef](#)]
19. Guerra, P.; Gonzalez, C.; Escauriaza, C.; Pizarro, G.; Pasten, P. Incomplete Mixing in the Fate and Transport of Arsenic at a River Affected by Acid Drainage. *Water Air Soil Pollut.* **2016**, *227*, 1–20. [[CrossRef](#)]
20. Kirat, G.; Aydin, N. Investigation of Metal Pollution in Moryayla (Erzurum) and Surrounding Stream Sediments, Turkey. *Int. J. Environ. Sci. Technol.* **2018**, *15*, 2229–2240. [[CrossRef](#)]
21. Ruiz, F.; González-Regalado, M.L.; Muñoz, J.M.; Abad, M.; Toscano, A.; Prudencio, M.I.; Dias, M.I. Distribution of Heavy Metals and Pollution Pathways in a Shallow Marine Shelf: Assessment for a Future Management. *Int. J. Environ. Sci. Technol.* **2014**, *11*, 1249–1258. [[CrossRef](#)]
22. Schemel, L.E.; Kimball, B.A.; Bencala, K.E. Colloid Formation and Metal Transport through Two Mixing Zones Affected by Acid Mine Drainage near Silverton, Colorado. *Appl. Geochem.* **2000**, *15*, 1003–1018. [[CrossRef](#)]
23. Allman, C.J.; Gómez-Ortiz, D.; Burke, A.; Amils, R.; Rodriguez, N.; Fernández-Remolar, D. Hydrogeochemical Variability of the Acidic Springs in the Rio Tinto Headwaters. *Water* **2021**, *13*, 2861. [[CrossRef](#)]
24. Biat, A.; Karbassi, A.R. Comparison of Controlling Mechanisms of Flocculation Processes in Estuaries. *Int. J. Environ. Sci. Technol.* **2010**, *7*, 731–736. [[CrossRef](#)]
25. Abarca, M.; Guerra, P.; Arce, G.; Montecinos, M.; Escauriaza, C.; Coquery, M.; Pastén, P. Response of Suspended Sediment Particle Size Distributions to Changes in Water Chemistry at an Andean Mountain Stream Confluence Receiving Arsenic Rich Acid Drainage. *Hydrol. Processes* **2017**, *31*, 296–307. [[CrossRef](#)]
26. Arce, G.; Montecinos, M.; Guerra, P.; Escauriaza, C.; Coquery, M.; Pastén, P. Enhancement of Particle Aggregation in the Presence of Organic Matter during Neutralization of Acid Drainage in a Stream Confluence and Its Effect on Arsenic Immobilization. *Chemosphere* **2017**, *180*, 574–583. [[CrossRef](#)] [[PubMed](#)]
27. Schwarz, C.; Cox, T.; van Engeland, T.; van Oevelen, D.; van Belzen, J.; van de Koppel, J.; Soetaert, K.; Bouma, T.J.; Meire, P.; Temmerman, S. Field Estimates of Floc Dynamics and Settling Velocities in a Tidal Creek with Significant Along-Channel Gradients in Velocity and SPM. *Estuar. Coast. Shelf Sci.* **2017**, *197*, 221–235. [[CrossRef](#)]
28. Droppo, I.G. Rethinking What Constitutes Suspended Sediment. *Hydrol. Processes* **2001**, *15*, 1551–1564. [[CrossRef](#)]
29. Shankar, M.S.; Pandey, M.; Shukla, A.K. Analysis of Existing Equations for Calculating the Settling Velocity. *Water* **2021**, *13*, 1987. [[CrossRef](#)]
30. Bigham, J.; Fitzpatrick, R.W.; Schulze, D. Iron Oxides. *Soil Mineral. Environ. Appl.* **2002**, *7*, 323–366.
31. Bigham, J.; Nordstrom, D.K. Iron and Aluminum Hydroxysulfates from Acid Sulfate Waters. *Rev. Mineral. Geochem.* **2000**, *40*, 351–403. [[CrossRef](#)]
32. Hogg, R. Flocculation and Dewatering. *Int. J. Miner. Processing* **2000**, *58*, 223–236. [[CrossRef](#)]
33. Adra, A.; Morin, G.; Ona-Nguema, G.; Menguy, N.; Maillot, F.; Casiot, C.; Bruneel, O.; Lebrun, S.; Juillot, F.; Brest, J. Arsenic Scavenging by Aluminum-Substituted Ferrihydrites in a Circumneutral PH River Impacted by Acid Mine Drainage. *Environ. Sci. Technol.* **2013**, *47*, 12784–12792. [[CrossRef](#)] [[PubMed](#)]
34. Burgos, W.D.; Borch, T.; Troyer, L.D.; Luan, F.; Larson, L.N.; Brown, J.F.; Lambson, J.; Shimizu, M. Schwertmannite and Fe Oxides Formed by Biological Low-PH Fe (II) Oxidation versus Abiotic Neutralization: Impact on Trace Metal Sequestration. *Geochim. Cosmochim. Acta* **2012**, *76*, 29–44. [[CrossRef](#)]
35. Ye, C.; Ariya, P.A.; Fu, F.; Yu, G.; Tang, B. Influence of Al(III) and Sb(V) on the Transformation of Ferrihydrite Nanoparticles: Interaction among Ferrihydrite, Coprecipitated Al(III) and Sb(V). *J. Hazard. Mater.* **2020**, *408*, 124423. [[CrossRef](#)]
36. Yukselen, M.A.; Gregory, J. The Effect of Rapid Mixing on the Break-up and Re-Formation of Floccs. *J. Chem. Technol. Biotechnol.* **2004**, *79*, 782–788. [[CrossRef](#)]
37. Concha, A.; Kynch, K. Theory of Sedimentation. In *Solid-Liquid Separation in the Mining Industry*; Concha, A.F., Ed.; Springer: Berlin/Heidelberg, Germany, 2014; pp. 97–118. ISBN 978-3-319-02484-4.
38. Major, J.J. *Hindered Settling BT-Encyclopedia of Sediments and Sedimentary Rocks*; Middleton, G.V., Church, M.J., Coniglio, M., Hardie, L.A., Longstaffe, F.J., Eds.; Springer: Dordrecht, The Netherlands, 2003; pp. 358–360. ISBN 978-1-4020-3609-5.
39. Derksen, J.J. Simulations of Hindered Settling of Flocculating Spherical Particles. *Int. J. Multiph. Flow* **2014**, *58*, 127–138. [[CrossRef](#)]
40. Vanoni Vito, A. *Sedimentation Engineering*; American Society of Civil Engineering: Reston, VA, USA, 2006; ISBN 978-0-7844-0823-0.
41. Bhargava, D.; Rajagopal, K. Differentiation between Transition Zone and Compression in Zone Settling. *Water Res.* **1993**, *27*, 457–463. [[CrossRef](#)]
42. Bian, J.; Wang, H.; Xiao, C.; Zhang, D. An Experimental Study on the Flocculating Settling of Unclassified Tailings. *PLoS ONE* **2018**, *13*, e0204230. [[CrossRef](#)] [[PubMed](#)]
43. Fritsch, F.N.; Carlson, R.E. Monotone Piecewise Cubic Interpolation. *SIAM J. Numer. Anal.* **1980**, *17*, 238–246. [[CrossRef](#)]
44. Ball, J.; Nordstrom, D.K. *User's Manual for WATEQ4F, with Revised Thermodynamic Data Base and Text Cases for Calculating Speciation of Major, Trace, and Redox Elements in Natural Waters*; US Geological Survey: Reston, VA, USA, 1991.

45. Kirk Nordstrom, D. Geochemical Modeling of Iron and Aluminum Precipitation during Mixing and Neutralization of Acid Mine Drainage. *Minerals* **2020**, *10*, 547. [[CrossRef](#)]
46. Caraballo, M.A.; Wanty, R.B.; Verplanck, P.L.; Navarro-Valdivia, L.; Ayora, C.; Hochella, M.F., Jr. Aluminum Mobility in Mildly Acidic Mine Drainage: Interactions between Hydrobasaluminite, Silica and Trace Metals from the Nano to the Meso-Scale. *Chem. Geol.* **2019**, *519*, 1–10. [[CrossRef](#)]
47. Grundl, T.; Delwiche, J. Kinetics of Ferric Oxyhydroxide Precipitation. *J. Contam. Hydrol.* **1993**, *14*, 71–87. [[CrossRef](#)]
48. Shammass, N. Coagulation and Flocculation. In *Physicochemical Treatment Processes. Handbook of Environmental Engineering*; Wang, L.K., Hung, Y.-T., Shammass, N.K., Eds.; Humana Press: Totowa, NJ, USA, 2005; Volume 3.
49. Mineralogy Database. Schwertmannite Mineral Data; 2009. Available online: <http://webmin.mindat.org/data/Schwertmannite.shtml#.Ys9zNTdBxPZ> (accessed on 31 May 2022).
50. Mineralogy Database. Jarosite Mineral Data; 2009. Available online: <http://webmineral.com/data/Jarosite.shtml#.Ys9zkjdBxPY> (accessed on 31 May 2022).
51. Mineralogy Database. Hydrobasaluminite Mineral Data; 2009. Available online: <http://www.webmineral.com/data/Hydrobasaluminite.shtml#.Ys9zxTdBxPY> (accessed on 31 May 2022).
52. Balistrieri, L.; Seal, R.R.; Piatak, N.M.; Paul, B. Assessing the Concentration, Speciation, and Toxicity of Dissolved Metals during Mixing of Acid-Mine Drainage and Ambient River Water Downstream of the Elizabeth Copper Mine, Vermont, USA. *Appl. Geochem.* **2007**, *22*, 930–952. [[CrossRef](#)]
53. Civeira, M.; Oliveira, M.L.S.; Hower, J.C.; Agudelo-Castañeda, D.M.; Taffarel, S.R.; Ramos, C.G.; Kautzmann, R.M.; Silva, L.F.O. Modification, Adsorption, and Geochemistry Processes on Altered Minerals and Amorphous Phases on the Nanometer Scale: Examples from Copper Mining Refuse, Touro, Spain. *Environ. Sci. Pollut. Res.* **2016**, *23*, 6535–6545. [[CrossRef](#)] [[PubMed](#)]
54. Cruz-Hernández, P.; Pérez-López, R.; Nieto, J.M. Role of Arsenic During the Aging of Acid Mine Drainage Precipitates. *Procedia Earth Planet. Sci.* **2017**, *17*, 233–236. [[CrossRef](#)]
55. Olias, M.; Nieto, J.M.; Sarmiento, A.M.; Ceron, J.C.; Canovas, C.R. Seasonal Water Quality Variations in a River Affected by Acid Mine Drainage: The Odiel River (South West Spain). *Sci. Total Environ.* **2004**, *333*, 267–281. [[CrossRef](#)]
56. Romero, L.; Alonso, H.; Campano, P.; Fanfani, L.; Cidu, R.; Dadea, C.; Keegan, T.; Thornton, I.; Farago, M. Arsenic Enrichment in Waters and Sediments of the Rio Loa (Second Region, Chile). *Appl. Geochem.* **2003**, *18*, 1399–1416. [[CrossRef](#)]
57. Dempsey, B.A.; Jeon, B.-H. Characteristics of Sludge Produced from Passive Treatment of Mine Drainage. *Geochem. Explor. Environ. Anal.* **2001**, *1*, 89. [[CrossRef](#)]